2006

Air-Side Performance Evaluation of Three Types of Heat Exchangers in Dry, Wet, and Periodic Frosting Conditions

Ping Zhang
University of Illinois at Urbana-Champaign

Predrag Hrnjak
University of Illinois at Urbana-Champaign

AIR-SIDE PERFORMANCE EVALUATION OF THREE TYPES OF HEAT EXCHANGERS IN DRY, WET AND PERIODIC FROSTING CONDITIONS

Ping Zhang [1], *P. S. Hrnjak[2]

[1]Visiting Scholar, M & IE Department, University of Illinois at Urbana-Champaign, Illinois, USA;
Zhejiang Vocational College of Commerce, Hangzhou, China. E-mail: apple682hz@yahoo.com

[2]M & IE Department, University of Illinois at Urbana-Champaign, Illinois, USA.
Tel: +1-217-244-6377; fax: +1-217-333-1942; e-mail: pega@uiuc.edu

ABSTRACT

The performances of three types of heat exchangers that use the louver fin geometry: 1. parallel flow parallel fin with extruded flat tubes heat exchanger (PF^2), 2. parallel flow serpentine fin with extruded flat tubes heat exchanger (PFSF) and 3. round tube wave plate fin heat exchanger (RTPF) have been experimentally studied under dry, wet and frost conditions and results are presented. The parameters quantified include air-side pressure drop, water retention on the surface of the heat changer, capacity for air face velocity 0.9, 2 and 3 m/s, air humidity 70% and 80%. The performances of three types of heat exchanger are compared and the results obtained are presented. The primary goal of this project is to explore the thermal hydraulic performance of PF^2 heat exchanger in refrigeration and heat pump systems. Using both the dip testing method and wind tunnel experiment assess the condensate drainage behavior of the air-side surface of these three heat exchanger types.

1. INTRODUCTION

The louvered-fin, flat-tube heat exchangers are finding wider application as performance, compactness and cost concerns continue to drive heat exchanger design. Many investigators have studied air-side heat transfer and pressure drop characteristics of louvered fin and flat tube heat exchangers. Davenport (1980) reported a comprehensive study of a non-standard variant of the flat tube and louvered corrugated heat exchangers. Achaichia and Cowell (1988) measured air-side performance using 15 samples with flat tube and louvered plate and found the same flow pattern proposed by Davenport. Dejong and Jacobi (1999) presented flow visualization, pressure drop, and mass transfer data for five louvered fin geometries, focused on the understanding of physical processes rather than the development of correlations. Webb and Jung (1992) studied the application of brazed aluminum heat exchangers to the residential air-conditioner. Chang and Wang (1996) performed experimental studies on the air-side characteristics of louvered fin heat exchangers. Kim and Bullard (2002) measured air-side heat transfer and pressure drop data using 30 different brazed aluminum heat exchangers with different louver fin geometrical parameters. Aoki et al. (1989) performed an experimental study on heat transfer characteristics of different louver fin arrays such as louver angles, louver and fin pitches. Zhong and Jacobi (2005) introduce a new method, dynamic dip testing, to assess the condensate drainage behavior of the air-side surface of compact heat exchangers.

The studies on the thermal hydraulic performance for the louvered fin heat exchangers have been performed by many investigators, but very few data exist on the study of folded louvered-fin-flat-tube heat exchangers under wet and frosting conditions. Most louvered fins they tested are plate-and-tube louver fin and corrugated louvered fin with triangular channel or with rectangular channel. The new design, parallel louvered fin with flat tubes was reported pretty seldom. This paper presents experimental results of the air-side pressure drop, capacity for three types of heat exchanger, which fins are parallel louver fin, serpentine louver fin and plate louver fin, under dry, wet, and frosting conditions with discussion.

2. TEST FACILITY AND OPERATION CONDITIONS

A specially designed and constructed wind tunnel (Figure 1) was placed inside an environmental chamber. The heat exchanger under testing is placed in the frame, which is located at the inlet to the wind tunnel. It is hung on a load cell to measure the accumulated frost. Flexible plastic film is used to connect the heat exchanger and the tunnel,

allowing the heat exchanger to move freely in the vertical direction for proper frost mass measurement. The transparent wind tunnel in environmental chamber allows visualization. Four pressure taps are placed on the low-pressure side of the heat exchanger and on both sides of the nozzles. Air temperatures are measured using two grids of double precision thermocouples at the inlet and exit of the heat exchanger. One grid including two type-T thermocouples (±0.2°C) is placed at the inlet of the tested heat exchanger in the place parallel to it. The other grid including four type-T thermocouples is placed at the outlet of the heat exchanger in the same fashion as inlet grid. For measuring the air dew point inlet and outlet temperature of the heat exchanger, the two sample points respectively are placed in the front of the exchanger and at the outlet of the nozzle.

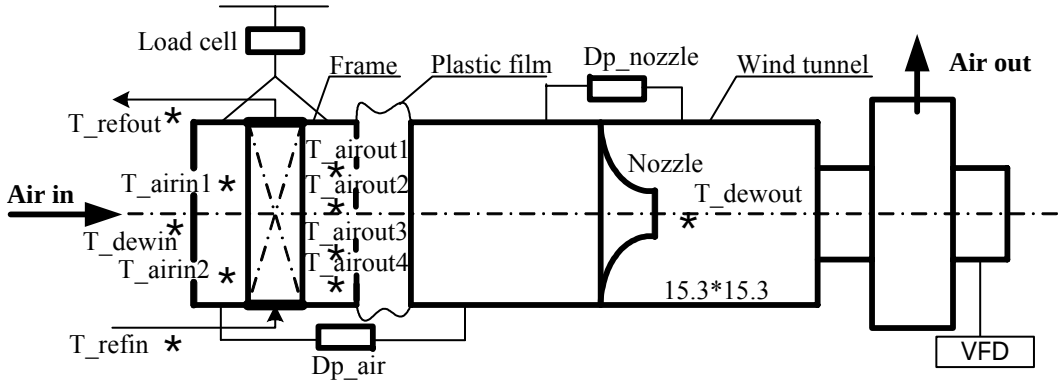

Figure 1: The open wind tunnel that are placed in the environmental chamber

The experimental facility used to test the heat exchangers under frosting and defrosting conditions is shown in Fig. 2. 100% ethyl alcohol supplied by a pump was used as the secondary refrigerant in the experimental loop. The alcohol flow was cooled by a R404A chiller system. A pre-cooler was included in the chamber to set the chamber to the desired temperature prior to the initiation of the experiment. The air temperature in the chamber is controlled using the first PID controller to regulate the power supplied to the heater located in the chamber according to a thermocouple sensor placed inside the chamber. Air humidification is provided by a steam, and the air inlet dew point is controlled using a General Eastern model D-2-SR chilled-mirror dew-point sensor (±0.2°C) and the second PID controller to regulate a solenoid valve in the steam line. Two chilled-mirror sensors of the same model were used to obtain humidity data upstream and downstream of the tested heat exchanger. Airflow is provided using a blower with a variable frequency drive so that three face velocities can be provided: 1m/s; 2m/s; 3m/s. The pressure drop across the nozzles can be measured using a Setra model 239 pressure transducer (±0.25 Pa) connected to pressure taps upstream and downstream of the nozzles and converted into the air mass flow rate. The pressure drop across the heat exchanger is measured using another Setra model 239 pressure transducer (±0.25 Pa) connected to static pressure taps. The secondary refrigerant temperature is controlled using the third PID controller to regulate power supplied to the heater located in the experimental loop. The secondary refrigerant temperatures are measured using immersion thermocouples probes (±0.2°C) at the inlet and exit of the heat exchanger. The secondary refrigerant flow rate is controlled using a variable frequency drive for the pump motor. A Coriolis-effect mass flow meter (±0.1%) is used to measure the mass flow rate of the refrigerant entering the heat exchanger.

At the initiation of an experiment, the secondary refrigerant was sent to the pre-cooler only until the chamber was cooled to the desired air condition. After achieving the desired chamber temperature and relative humidity, the refrigerant was diverted to the test heat exchanger, and data were collected. Experiments are operated in dry, wet and frosting conditions at the face velocities of 0.9 m/s, 2 m/s and 3 m/s. All test conditions are given in Table 1. In the dry condition, the experiment was conducted under dry surface conditions i.e. no water condensed during the experiment. It should be noted that during the course of an experiment in wet condition or frosting condition the face velocity decreased, owing to the increase in air-side pressure drop associated with water deposition or frost deposition. In the frost condition, the experiments are conducted at constant air-inlet temperature, refrigerant-inlet temperature, air inlet humidity, refrigerant mass flow rate, and blower frequency. When the air-side pressure drop increase to three or five times its initial value, defrost is initiated. A warm liquid refrigerant at room temperature 20 °C is used to melt the frost. The length of the defrost cycle was varied to come to period sufficient for water after defrost to be removed. The criterion was that air-side pressure drop at the beginning of the cycle was repeatable. Valves are switched and the refrigeration cycle begins. The system goes through five cycles of defrost and refrost.

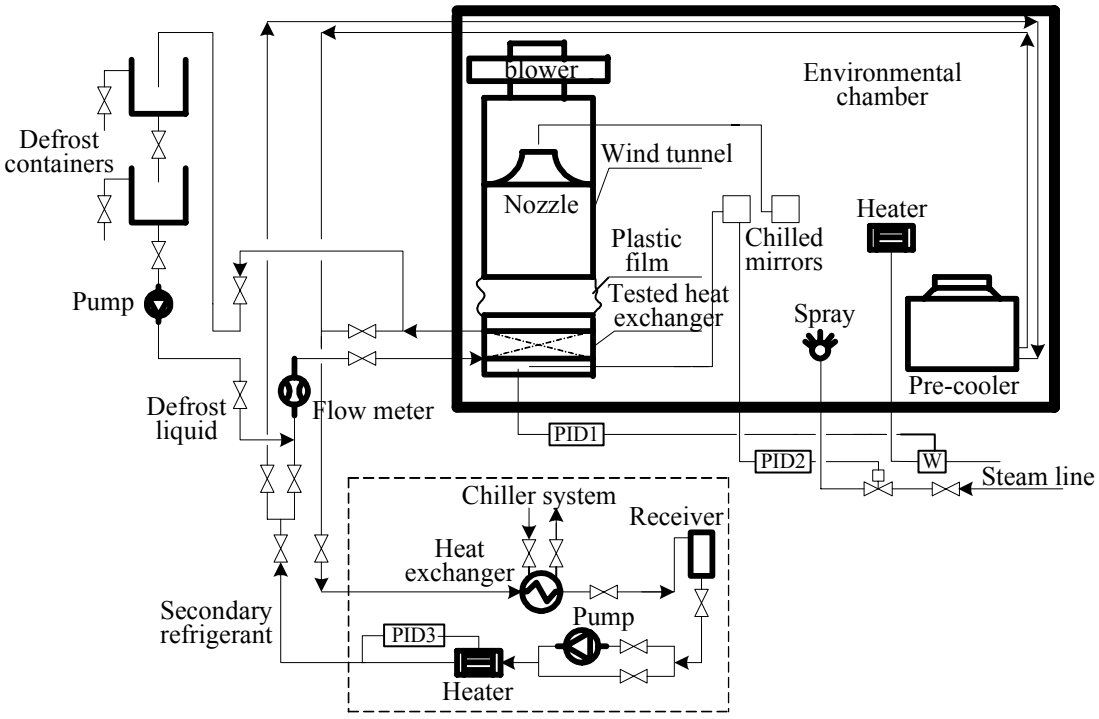

Figure 2: Experimental facility schematic

Table 1: Test conditions

Dry Condition	Air inlet temperature	44 °C
	Refrigerant inlet temperature	20 °C
	Air inlet dew point temperature	16.8 °C
	Air face velocity	0.9, 2, 3 m/s
Wet Condition	Air inlet temperature	35 °C
	Refrigerant inlet temperature	1 °C
	Air inlet dew point temperature	26.5 °C
	Initial air face velocity	0.9, 2, 3 m/s
Frosting condition	Air inlet temperature	0 °C
	Refrigerant inlet temperature	-14.5 °C
	Relative humidity	70%; 80%
	Initial air face velocity	0.9, 2, 3 m/s
	Air pressure drop	Three or five times initial value
	Defrost time	3 min
	Defrost temperature	20°C

3. THE TYPES OF HEAT EXCHANGERS EXPLORED

The photos of three HX types, PF parallel fins and PF serpentine fins and RT plate fin, used in this study are given in Figure 3. All three have same fin pitch (16 fpi), same louver pitch and same face area. The fin types tested were parallel fin, serpentine fin and plate fin. PF^2 and PFSF heat exchangers have basically the same dimensions, which are 152 mm length by 149 mm height by 21 mm width, and differ only in fin type (parallel fin and serpentine). PF^2 and PFSF were single-row heat exchanger with 19 mm tube major by 1.9 mm tube minor flat tube, while RTPF heat exchanger were two-row heat exchanger with the outside diameter of 9.5 mm round tubes. All three heat exchanger structures are shown in Figures 4, 5 and 6.

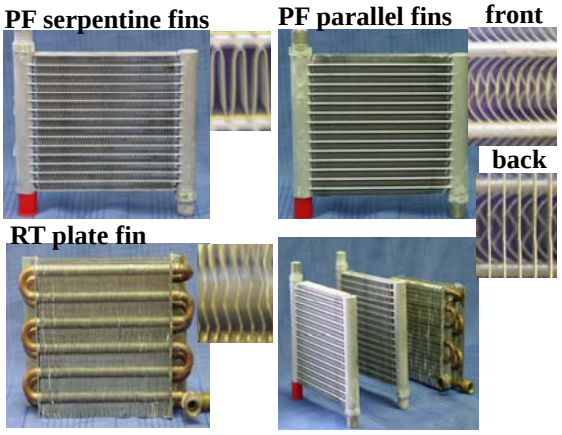

Figure 3: Three HX types – photos

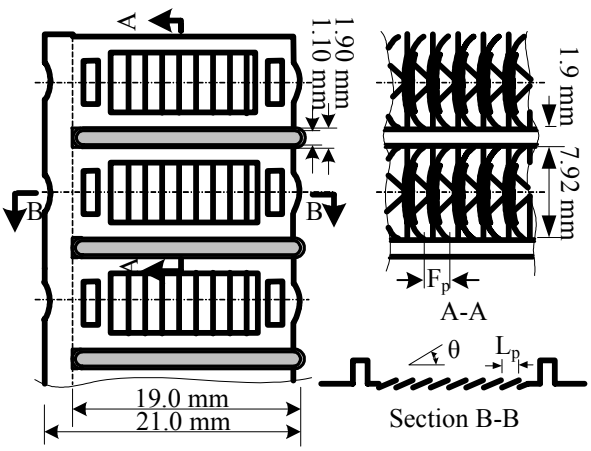

Figure 4: Structure of PF^2 in air-side

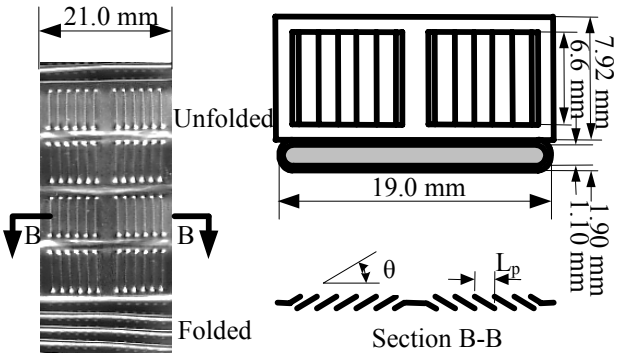

Figure 5: Structure of PFSF in air-side

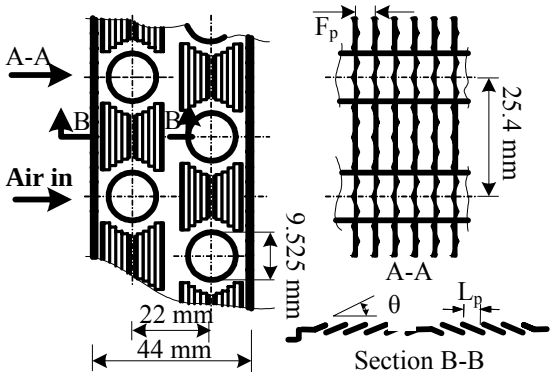

Figure 6: Structure of RTPF in air-side

4 . DATA REDUCTION METHOD

Heat transfer rate required for the calculation of air-side heat transfer coefficient can be expressed as

$$Q = (Q_{ref} + Q_{air})/2 \quad (1)$$

Where Q_{ref} and Qair are heat transfer rates of refrigerant and air side, respectively.

$$Q_{ref} = M_{ref} C_{pr} (T_{r,out} - T_{r,in}) \quad (2)$$

$$Q_{air} = M_{air} (h_{a,in} - h_{a,out}) \quad (3)$$

Where M_{ref} and M_{air} are the flow rate of the refrigerant and the air, C_{pr} is the specific heat of the refrigerant, $T_{r,out}$ and $T_{r,in}$ are the temperatures of the refrigerant inlet and outlet, $h_{a,in}$ and $h_{a,out}$ are the enthalpy of the air inlet and outlet.

Effectiveness and NTU method can be used for obtaining overall heat transfer coefficient (UA).

$$\varepsilon = 1 - \exp\left[\frac{NTU^{0.22}}{C_r}\left\{\exp\left(-C_r NTU^{0.78}\right) - 1\right\}\right] \quad (4)$$

Where

$$\varepsilon = Q / Q_{max}$$

$$Q_{\max} = C_{\min} \times (T_{a,in} - T_{r,in})$$

$$C_r = \frac{(MC_p)_{\min}}{(MC_p)_{\max}}$$

We can obtain overall heat transfer coefficient (UA) for the heat exchanger as:

$$UA = (MC_p)_{\min} NTU \tag{5}$$

5. RESULTS AND DISCUSSIONS

5.1 Comparative analysis between three types of heat exchangers

Three types of heat exchangers were explored: parallel flow parallel fin (PF^2), parallel flow serpentine fin (PFSF) and round tube plate fin (RTPF) as presented in Figures 3 through 6. All three have same fin pitch, face area and were tested under the same conditions in the same test facility. Heat exchangers PF^2 and PFSF have the same volume while RTPF is more than twice deep and thus volume is more than two times greater. It should be noted that for the same fin pitch PF^2 heat exchanger accommodates slightly more surface area than PFSF heat exchanger due to fin bending. It is designed to have a specific plate-fin in the back that allows water to fall down at the back side of trailing edge. This section presents the results and comparisons of the pressure drop, capacity between these three heat exchangers when tubes are placed horizontally (see Figure 3). Other orientations will be presented later in the paper.

5.1.1 Dry operation

Pressure drops (Figure 7) show almost the same specific value per heat exchanger depth; both PF^2 and PFSF are the same while RTPF is twice due to greater depth. PF^2 and PFSF are very close in heat transfer UA (see Figure 8) with PFSF showing slightly better (up to 5%) performance at 3 m/s. Higher UA value for RTPF structure is due to greater volume and air side surface area. Apparently, slightly lower comparative performance of PF^2 vs. PFSF is due to greater air side surface for the same fin pitch and RT plate fin heat exchanger is worse than both other geometries.

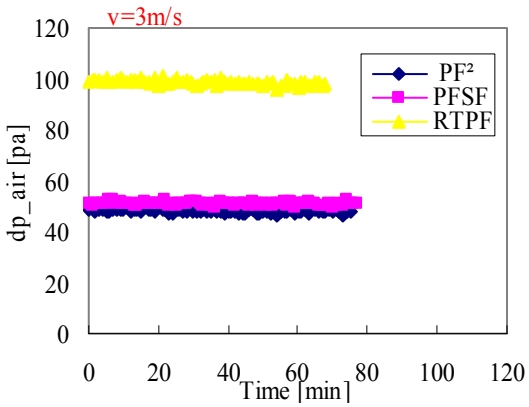

Figure 7: Air-side pressure drop in dry condition

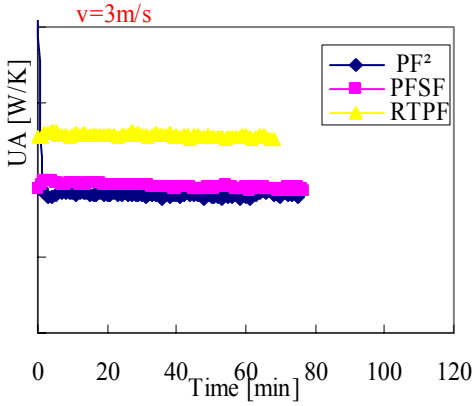

Figure 8: Heat transfer (UA) in dry condition

5.1.2 Wet operation

Diagrams in Figure 9 clearly identify that drainage in PF^2 is significantly better than PFSF and shows pressure drop for wet conditions is consistently higher than that for dry conditions in the same face velocity. Their pressure drop incremental rates per unit air-side heat transfer are shown in Figure 10. It can be observed from Figure 10 that PFSF heat exchanger has the most incremental rate of pressure drop per unit air-side heat transfer area (due to the most water per unit air-side heat transfer area retained on the surface of PFSF heat exchanger), followed by PF^2 and RTPF, and the incremental rate of pressure drop decreases with face velocity. That is probably due to higher face velocity improves condensate drainage as air shear force increases. At low velocities, the airflow forces are insufficient to push condensate to the exit face, and all drainage is down the fins and tubes. However, when the velocity is high, shear and pressure can cause condensate to flow to the exit face and drain more water down the fins and tubes. If the

air velocity is sufficient high, then some of the condensate will be separated from the coil and become entrained as droplets in the downstream flow.

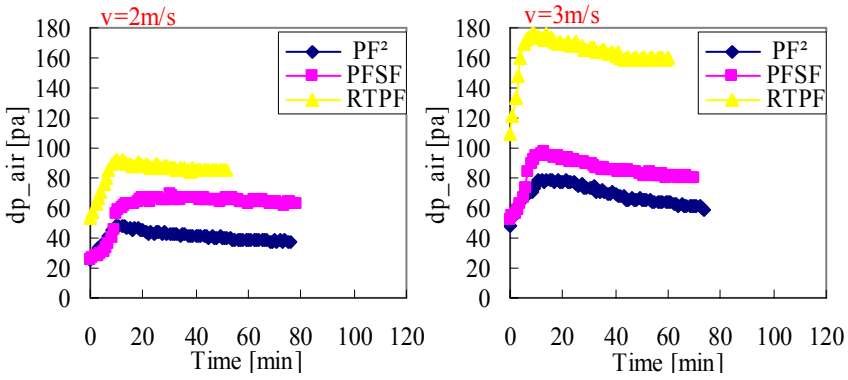

Figure 9: Air-side pressure drop in wet condition

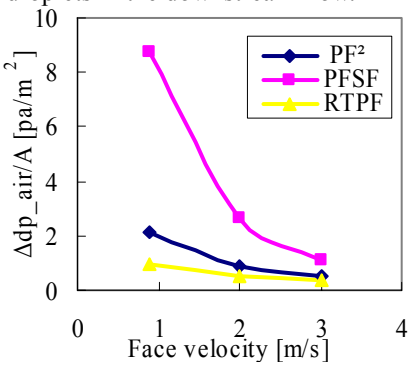

Figure 10: Incremental rate of pressure drop per unit air-side heat exchange as a function of face velocity

Dip test for the three heat exchangers had been conducted to measure the maximum amount of water retention on the heat exchanger, In which method (see Figure 11), a heat exchanger is submerged in a tank while suspended on a mass balance; the water level in the tank is suddenly reduced and the weight of the heat exchanger is measured as a function of time. The dip test results in the form of mass per unit air-side heat transfer area as a function of time are shown in Figure 11. By comparing the results from dip testing to wind-tunnel experiments for the same heat exchangers, the results from dip testing can confirm these findings, which is the drainage in PF^2 heat exchanger is significantly better than PFSF heat exchanger. It should be noted that in this comparison all tubes are horizontal.

Differences in draining and air side pressure drop did not significantly affect ranking in heat transfer (see Figure 12): PF^2 heat exchanger is just slightly behind PFSF heat exchanger while RTPF heat exchanger is lowest performance.

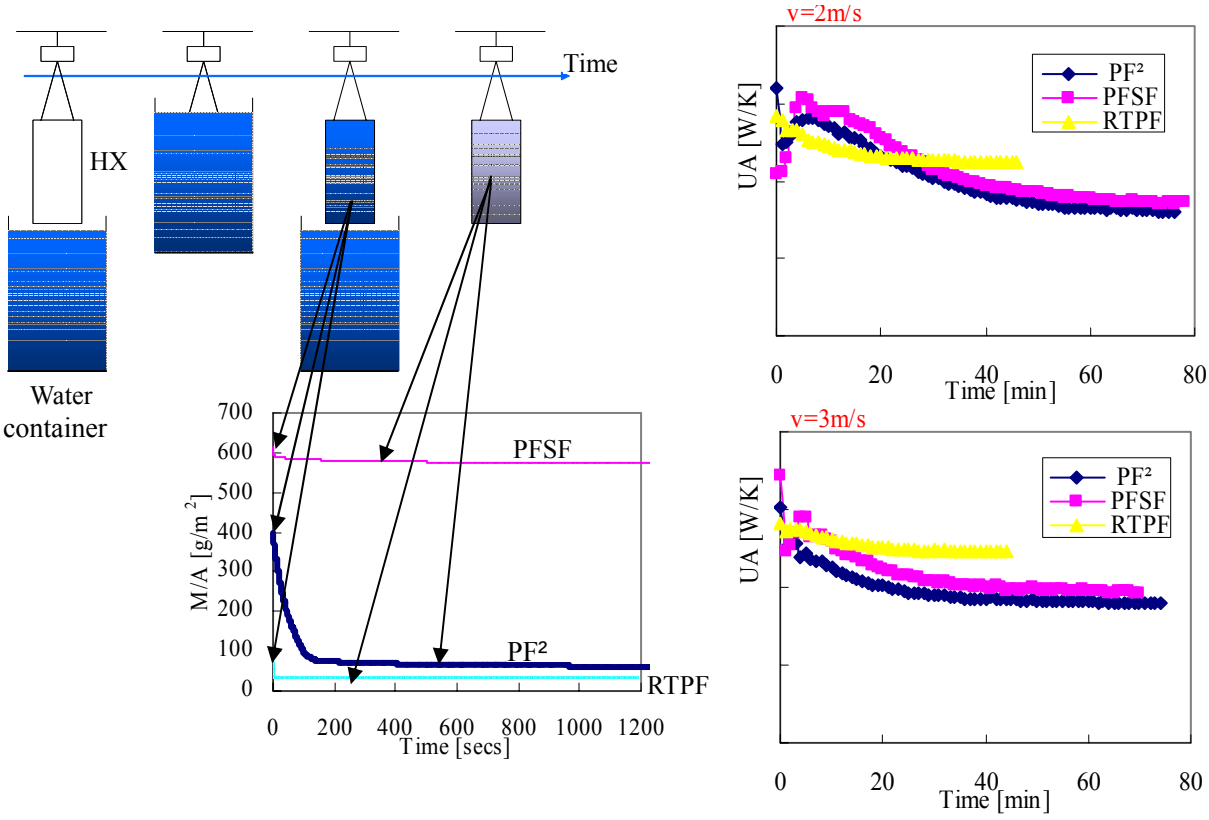

Figure 11: The mass of water retained on the coil unit air-side heat transfer area is shown as a function of time using dip test

Figure 12: Heat transfer (UA) in wet operation

5.1.3 Frosting operation

It takes several refrosting cycles for heat exchanger to come to repetitive condition due to build up of retained water after defrost (see the line of pressure drop after defrost going up in Figure 13). Figures 13 -14 present elements of performance for three heat exchanger types in first five frost cycles. When compared to PF^2 and PFSF, round tube heat exchanger shows the longest refrigeration time, defined by five fold increase of air side pressure drop (see Figure 13). This is the consequence of much greater surface area and thus thinner frost layer for almost the same dehumidification capacity. Air-side pressure drop in PF^2 heat exchanger increases slower (see Figure 13), thus allowing for longer refrigeration cycle than in PFSF. Defrost appears to be the same as in PFSF. Heat transfer in frosting shows the same trend (see Figure 14) as in wet operation in conditions explored.

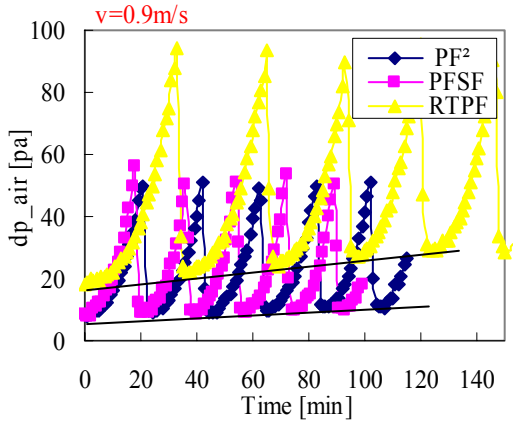

Figure 13: Air-side pressure drop in frosting operation

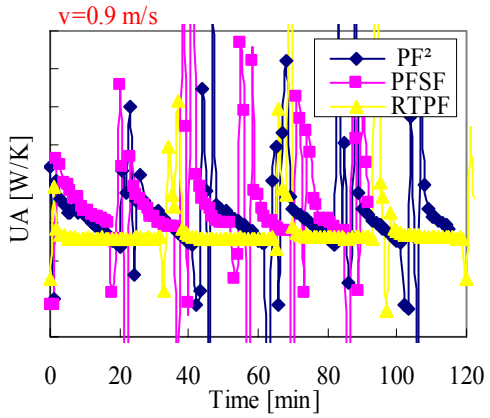

Figure 14: Heat transfer (UA) in frosting operation

5.2. Comparative analysis between PF^2 with horizontal tubes and PFSF with vertical tubes

The vertical tube orientation of PFSF heat exchanger and the horizontal tube orientation of PF^2 are compared. In the wet condition (see Figures 15), PF^2 with horizontal tubes orientation drains slightly better than PFSF with vertical tube orientation. The dip test data (see Figure 16) confirms the water retention in the PF^2 with horizontal tubes orientation is the slightly lower than the PFSF with vertical tubes orientation. PFSF with vertical tube orientation has a higher capacity (UA) (see Figure 17). In the frosting condition, the PF^2 with horizontal tubes orientation is able to operate longer before defrosting is necessary (see Figure 18), and has lower capacity (UA) (see Figure 19).

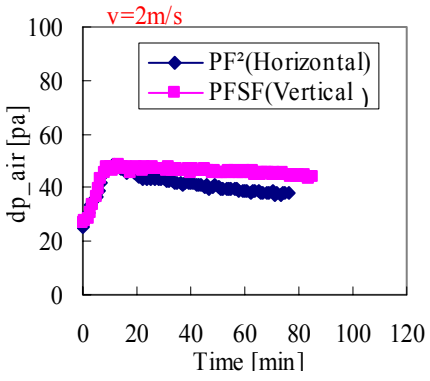

Figure 15: Air-side pressure drop In wet condition

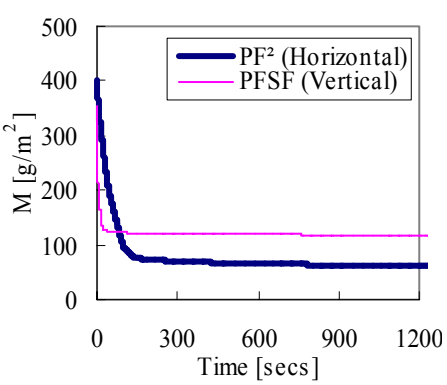

Figure 16: dip test data

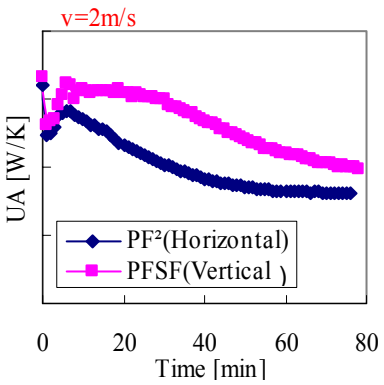

Figure 17: Heat transfer (UA) in wet operation

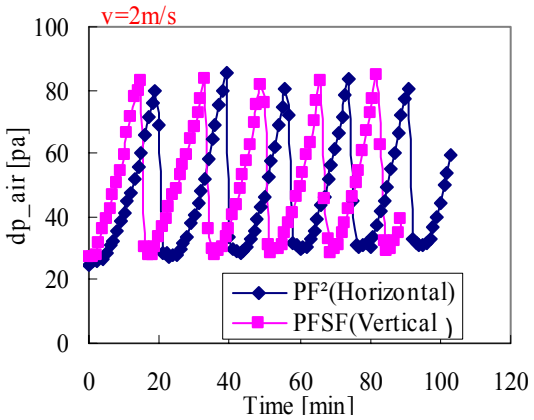

Figure 18: Air-side pressure drop in frosting condition

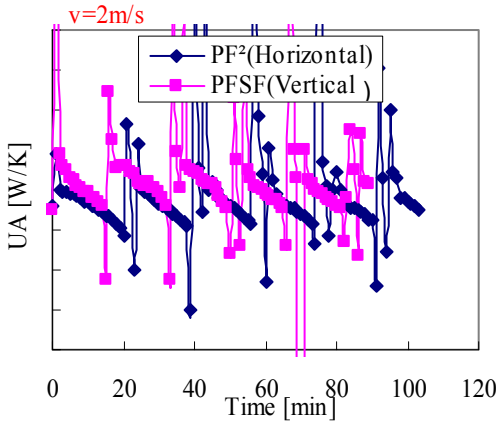

Figure 19: Heat transfer (UA) in frosting condition

6. CONCLUSIONS

1 . The capacity of the PF^2 heat exchanger is very close to the PFSF heat exchanger in the same volume for the same fin pitch and far better than round tube plate fin heat exchanger when all three type heat exchangers were placed in tube horizontally, and the heat transfer coefficient of PF^2 is just slightly behind PFSF while RTPF heat exchanger is the lowest.

2. Good drainage of water for PF^2 heat exchanger with horizontal tubes is due to a specific plate-fin design that allows water to fall down at the back side of its trailing edge. specifically: (1) the drainage in PF^2 heat exchanger is significantly better than PFSF heat exchanger and RTPF heat exchanger when all tubes are horizontal; (2) PFSF heat exchanger in vertical orientation has better drainage than in horizontal, but PF^2 heat exchanger in horizontal orientation still has better drainage that PFSF heat exchanger in vertical orientation.

3 . Higher face velocity can improve condensate drainage for three types of heat exchanger.

ACKNOWLEDGEMENTS

We are grateful for financial support from Modine Manufacturing Company, Greg Kohler, Kevin Mercer and for technical support from the Air Conditioning and Refrigeration Center (ACRC) at the University of Illinois.

REFERENCES

1. Davenport CJ., 1980, Heat transfer and fluid flow in louvered triangular ducts. PhD thesis, Department of Mechanical Engineering, Lanchester Polytechnic.
2. A. Achaichia and T.A. Cowell, 1988, Heat transfer and pressure drop characteristics of flat and louvered plate fin surface. Exp. Thermal and Fluid Sci. 1, pp. 147–157.
3. Dejong, N. C. and Jacobi, A. M., 1999, Flow, heat transfer, and pressure drop Interactions in Louvered-fin Arrays. ACRC TR-146, Air Conditioning and Refrigeration Center (ACRC), University of Illinois at Urbana-Champaign.
4. Webb R. L. and Jung, S.H., 1992, Air-side performance of echanced brazed aluminium heat exchangers, ASHRAE Trans. 98, Pt 2, 391-401.
5. Chang, Y. and Wang, C., 1996, Air-side performance of brazed aluminum heat exchangers. Journal of Enhanced Heat Transfer 3(1), pp. 15–28.
6. Kim, M.-H. and Bullard, C. W., 2002, Air-side performance of brazed aluminum heat exchangers under dehumidifying conditions. Int. J. Refrigeration 25(5), 641-652.
7. Aoki, H., Shinagawa, T. and Suga, K.K., 1989, An experimental study of the local heat transfer characteristics in automotive louvered fins. Exp. Thermal Fluid Sci. 2, 293-300.
8. Zhong, YF, Joardar, A., Gu, ZP, Park, YG, and Jacobi, A. M., 2005, Dynamic dip testing as a method to assess the condensate drainage behavior from the air-side surface of compact heat exchangers. Experimental Thermal and

Fluid Science Volume 29, Issue 8, Pages 957-970.